

Surface modification of $\text{LiNi}_{0.5}\text{Mn}_{1.5}\text{O}_4$ cathodes with ZnAl_2O_4 by a sol–gel method for lithium ion batteries



Yongho Lee^{a,b}, Junyoung Mun^c, Dong-Won Kim^b, Joong Kee Lee^a, Wonchang Choi^{a,*}

^a Center for Energy Convergence Research, Korea Institute of Science and Technology, Hwarangno 14-gil 5, Seongbuk-gu, Seoul 136-791, Republic of Korea

^b Department of Chemical Engineering, Hanyang University, 17 Haengdang-dong, Seongdong-gu, Seoul 133-791, Republic of Korea

^c Energy Storage Group, Samsung Advanced Institute of Technology, Samsung Electronics Co., Ltd., 14-1, Nongseo-dong, Giheung-gu, Yong-in si, Gyeonggi-do 446-712, Republic of Korea

ARTICLE INFO

Article history:

Received 15 August 2013

Received in revised form 10 October 2013

Accepted 15 October 2013

Available online 6 November 2013

Keywords:

Lithium ion battery

Lithium nickel manganese oxide

Surface modification

Zinc aluminate coating

ABSTRACT

The 5V spinel $\text{LiNi}_{0.5}\text{Mn}_{1.5}\text{O}_4$ cathodes have been surface-modified with ZnAl_2O_4 by a sol–gel method and characterized by X-ray diffraction, high-resolution transmission electron microscopy, and electrochemical measurements. Although the pristine electrode experienced the prominent degradation after the storage test at 60 °C in the intervals of cycling test at room temperature, the ZnAl_2O_4 -coated $\text{LiNi}_{0.5}\text{Mn}_{1.5}\text{O}_4$ cathode exhibited the significant capacity retention even after storing at elevated temperatures. The X-ray photoelectron spectroscopy data reveals that the improved electrochemical performances of surface-coated cathode are mostly due to the suppressed side reaction between the cathode and the electrolyte especially at the high-temperature environment. Differential scanning calorimetry showed that the decreased heat evolution could be found with the surface-modified cathode. Our experimental findings suggest a direction to the further development of cathode materials which are enduring to the highly oxidized state and high-temperature environment.

© 2013 Published by Elsevier Ltd.

1. Introduction

Lithium ion batteries have been successful for portable electronic devices such as cell phones and laptop computers due to their higher energy density compared to other rechargeable systems [1]. In addition to those achievements, aggressive research has recently been focused on the development and optimization of advanced cathode materials for electric vehicles (EV) and hybrid electric vehicles (HEV) [2]. However, the high cost, toxicity, and safety issues associated with the currently used layered LiCoO_2 cathode remain as an impediment for employing the lithium ion battery technology for EV and HEV application. In this regard, various lithium transition metal oxides and phosphates have been investigated to replace the LiCoO_2 cathode materials [3–6]. Among the various cathode materials, spinel $\text{LiNi}_{0.5}\text{Mn}_{1.5}\text{O}_4$ cathode employing inexpensive Mn is appealing as it gives higher energy density originated from the high voltage plateau around 4.7V compared to the conventional spinel LiMn_2O_4 system [7–13]. Unfortunately, spinel $\text{LiNi}_{0.5}\text{Mn}_{1.5}\text{O}_4$ cathodes have drawbacks, especially at the elevated temperatures, mainly owing to the highly oxidized environment of Ni^{4+} and subsequent side reaction between the cathode and the electrolyte especially during the charge process

[14–25]. To overcome these disadvantages, many researchers have recently focused on the stabilization of $\text{LiNi}_{0.5}\text{Mn}_{1.5}\text{O}_4$ cathodes by the surface-coating with the various oxides and phosphates such as ZnO [26,27], ZrO_2 [28], ZrP_2O_7 [28], Al_2O_3 [27,29], AlPO_4 [27], Bi_2O_3 [27,29], SiO_2 [30], and BiOF [31]. These previous literatures have reported that the surface-modifications using inorganic materials are effective to enhance the electrochemical performances and the thermal stability of the high-voltage $\text{LiNi}_{0.5}\text{Mn}_{1.5}\text{O}_4$ cathode system, confirming the several functions of coating layer such as the protection of the active material from HF attack, reduction of an increase in interfacial impedance, and pH environment control between the cathode and the electrolyte [26–31].

To utilize these multi-functional advantages of surface-modifications, we introduced the novel coating layer of zinc aluminate with the spinel structure because the ZnAl_2O_4 is known to possess and offer the low surface acidity characteristics, hydrophobic behavior, high thermal and chemical stability, and high mechanical resistance in transparent conductor, dielectric materials and catalyst applications [32–34]. In the present study, to the best of our knowledge, ZnAl_2O_4 is prepared for the first time as a coating material by a sol–gel method with citric acid to improve the electrochemical performances as well as the thermal stability of $\text{LiNi}_{0.5}\text{Mn}_{1.5}\text{O}_4$ cathodes. To identify and understand the physical and electrochemical properties of the ZnAl_2O_4 -coated $\text{LiNi}_{0.5}\text{Mn}_{1.5}\text{O}_4$ cathodes, various analytical techniques are employed. The surface-modified $\text{LiNi}_{0.5}\text{Mn}_{1.5}\text{O}_4$ cathode

* Corresponding author. Tel.: +82 2 958 5253; fax: +82 2 958 5229.

E-mail addresses: wonchangchoi@kist.re.kr, unchaeng@gmail.com (W. Choi).

system demonstrates the enhanced electrochemical performances compared to those of pristine $\text{LiNi}_{0.5}\text{Mn}_{1.5}\text{O}_4$ especially under elevated temperature conditions.

2. Experimental

For the parent cathode materials, $\text{LiNi}_{0.5}\text{Mn}_{1.5}\text{O}_4$ particles with an average size of ca. 7–10 μm were obtained from the Tanaka Chemical Corporation (Japan). The sol–gel method was utilized to prepare both the ZnAl_2O_4 oxides and ZnAl_2O_4 -coated $\text{LiNi}_{0.5}\text{Mn}_{1.5}\text{O}_4$ particles. To synthesize the ZnAl_2O_4 oxides, stoichiometric amount of $\text{Zn}(\text{NO}_3)_2 \cdot 6\text{H}_2\text{O}$ (Sigma–Aldrich) and $\text{Al}(\text{NO}_3)_3 \cdot 9\text{H}_2\text{O}$ (Sigma–Aldrich) were dissolved in distilled water. Then, the citric acid and ethylene glycol were added slowly to the solution, in which the mole ratio of citric acid to total metal ions was fixed at 4. In the case of ZnAl_2O_4 -coated samples, $\text{LiNi}_{0.5}\text{Mn}_{1.5}\text{O}_4$ particles were added at this point with vigorous stirring. The amount of zinc and aluminum nitrate for surface-coating was calculated with an intention to incorporate the 3 wt% of ZnAl_2O_4 in the final products compared to the parent $\text{LiNi}_{0.5}\text{Mn}_{1.5}\text{O}_4$ particles. Subsequently, the solution was stirred at 80 °C to form a viscous transparent gel, and the gel was preheated at 180 °C for the further esterification. The resulting precursors were annealed at 900 °C for 12 h. X-ray powder diffraction (XRD) data was collected with a Rigaku X-ray diffractometer using monochromatic $\text{Cu K}\alpha$ radiation at 40 kV and 100 mA to identify the phases in samples. Diffraction patterns were recorded with a scan speed of 1° per minute between 10° and 80°. The morphology of the pristine and surface-modified $\text{LiNi}_{0.5}\text{Mn}_{1.5}\text{O}_4$ powders was characterized by high-resolution transmission electron microscopy (HR-TEM, FEI company-Tecnaig2).

The electrochemical performances of the cathode materials were evaluated with CR2032 coin cells consisting of cathode, anode, electrolyte, and polypropylene separator. The cathodes were prepared by mixing 92 wt% cathode powders with 4 wt% Denka Black and 4 wt% binder (polyvinylidene fluoride) in a solvent (*N*-methyl-*w*-pyrrolidone). The slurry was uniformly pasted onto an Al foil, then dried at 120 °C in a vacuum oven and then pressed under a constant load. Lithium metal was used as the counter electrode, and 1.3 M LiPF_6 in a mixture of ethylene carbonate and ethyl methyl carbonate was employed as the electrolyte. Galvanostatic cycling measurement was carried out by repeating the charging and discharging process at C/10 or 1C rate between 3.5 and 4.9 V versus Li/Li^+ at room temperature. All the charging process was performed at a constant current mode up to 4.9 V, followed by a constant voltage mode until the current drops close to 0.05C values. The storage performances were carried out at fully charged state and

Table 1

Comparison of the lattice parameters of the pristine $\text{LiNi}_{0.5}\text{Mn}_{1.5}\text{O}_4$ and ZnAl_2O_4 -coated $\text{LiNi}_{0.5}\text{Mn}_{1.5}\text{O}_4$ from a least square method.

Sample	Lattice parameter (Å)
Pristine $\text{LiNi}_{0.5}\text{Mn}_{1.5}\text{O}_4$	8.165(7)
ZnAl_2O_4 -coated $\text{LiNi}_{0.5}\text{Mn}_{1.5}\text{O}_4$	8.165(1)

elevated temperatures such as 60 °C. To investigate the surface state of the cathodes, X-ray photoelectron spectroscopy (XPS, Ulvac-PHI, PHI 5000 VersaProbe) was performed under Ar atmosphere. For the XPS experiment, all cells were carefully disassembled at fully discharged state inside the glove box to avoid any contamination of the surface state of the cathodes. The thermal stability of the cathodes was evaluated with differential scanning calorimetry (DSC, TA Instruments Auto Q20) analysis for the fully charged electrodes up to 4.9 V versus Li/Li^+ . The samples typically include 5 mg of the scraped electrode materials and 5 μl of electrolyte inside the stainless-steel high-pressure capsules. Then, the capsules were hermetically sealed to prevent leakage of the pressurized solvents. All the samples were prepared inside glove box under Ar atmosphere to prevent a possible contamination.

3. Results and discussion

In order to examine the possibility of the surface modification with ZnAl_2O_4 on the parent cathode materials, we have first prepared the ZnAl_2O_4 oxides using a sol–gel method at 900 °C. As shown in Fig. 1a, the XRD pattern of the synthesized ZnAl_2O_4 oxides exhibits that the main reflection characteristics of spinel structure as well as the high crystallinity were well-developed without any impurity phase [35]. After the preliminary experiment mentioned above, surface-coating with the ZnAl_2O_4 oxides was carried out on the parent $\text{LiNi}_{0.5}\text{Mn}_{1.5}\text{O}_4$ powders as described in the experimental section. The XRD patterns presented in Fig. 1b and c reveal that the surface-modification using a sol–gel method and heat treatment at 900 °C does not cause prominent bulk change of parent materials in the crystal lattice, and the lattice parameters calculation using a least square method in Table 1 exhibit the little difference in lattice parameter, indicating that zinc or aluminum ions are not incorporated into the spinel lattice during surface-modification process, suggesting that the introduction of zinc and aluminum including heat treatment at high temperatures do not influence the parent cathode materials. Although we intend to introduce the crystalline coating layer of ZnAl_2O_4 , no clear reflections of ZnAl_2O_4 corresponding to the spinel peaks were found from the XRD patterns possibly due to the small amount of coating materials around 3 wt% compared to parent cathode materials.

To identify the physicochemical feature of surface modification with the crystallized ZnAl_2O_4 on the parent cathode materials, we have examined an analysis of morphology and crystal structure of cathodes using the high-resolution TEM with a careful observation in Fig. 2. The TEM image of ZnAl_2O_4 -modified sample shown in Fig. 2b exhibits that the smooth or island-typed coating layers with a thickness less than 100 nm were formed on the surface of the cathode materials compared to the surfaces of pristine cathode materials presented in Fig. 2a. The elements of the coating layers at the designated spot of A and B in Fig. 2b were confirmed by TEM-EDS analysis, as shown in Fig. 2c and d. It is known that the synthesis of ZnAl_2O_4 above 600 °C often leads to the zinc evolution due to the volatile characteristics of zinc ion, especially, at a long heat treatment with the solid-state method. The clear peak of zinc element and the qualitative peak ratio between zinc and aluminum element reveals that the Zn–Al–O coating layer successfully formed. Also, the spot patterns presented in Fig. 2e and f indicate

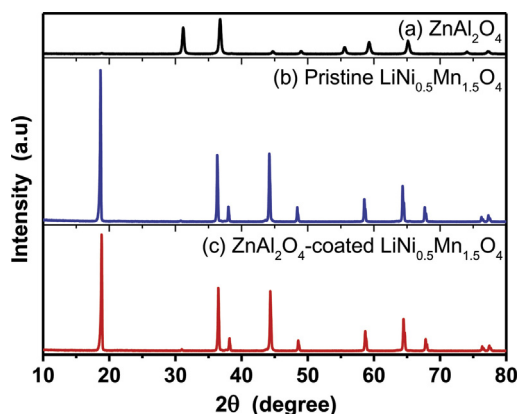


Fig. 1. Powder XRD patterns of (a) ZnAl_2O_4 , (b) $\text{LiNi}_{0.5}\text{Mn}_{1.5}\text{O}_4$, and (c) ZnAl_2O_4 -coated $\text{LiNi}_{0.5}\text{Mn}_{1.5}\text{O}_4$.

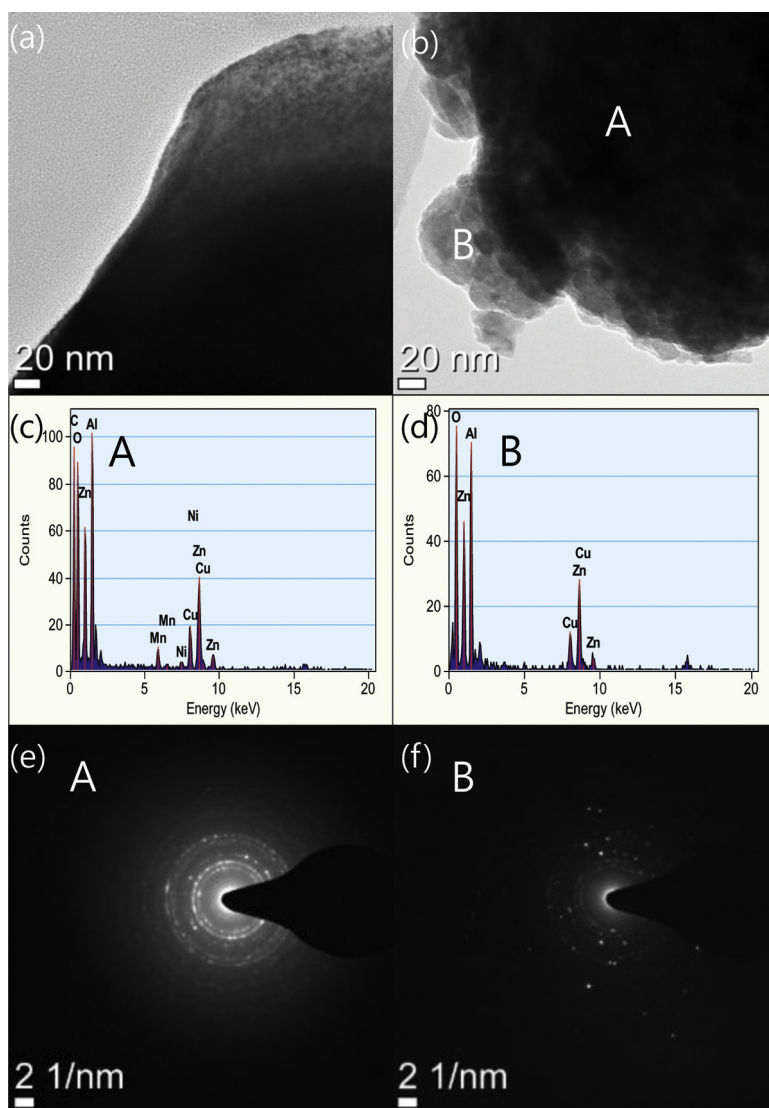


Fig. 2. HR-TEM images of (a) pristine $\text{LiNi}_{0.5}\text{Mn}_{1.5}\text{O}_4$ and (b) ZnAl_2O_4 -coated $\text{LiNi}_{0.5}\text{Mn}_{1.5}\text{O}_4$ synthesized by a sol-gel method. EDX results and electron diffraction pattern of selected area- (b) ZnAl_2O_4 -coated $\text{LiNi}_{0.5}\text{Mn}_{1.5}\text{O}_4$.

the crystalline or multi-crystalline phase characteristics of the coating layers, suggesting that surface coating with the spinel ZnAl_2O_4 were successfully achieved on the cathode powders with a sol-gel based synthesis method.

Fig. 3 represents the charge and discharge profiles of the pristine and ZnAl_2O_4 -coated $\text{LiNi}_{0.5}\text{Mn}_{1.5}\text{O}_4$ cathodes evaluated at $C/10$ rate between 3.5 and 4.9 V for the first cycle. Both cathodes deliver the similar capacities around 130 mA h g^{-1} although the surface-modified sample exhibits the slightly decreased capacity values around 127 mA h g^{-1} . Also, the pristine and ZnAl_2O_4 -coated electrodes provide the typical flat portion of voltage profiles which correspond to the reflection of $\text{Ni}^{2+}/\text{Ni}^{4+}$ redox couple around 4.7 V and $\text{Mn}^{3+}/\text{Mn}^{4+}$ redox couple around 4.0 V, indicating that the surface modification utilizing ZnAl_2O_4 oxides does not involve the additional electrochemical reaction with lithium ion during the charge-discharge process.

The cyclability data of the pristine and surface-modified electrodes evaluated at 1C rate is demonstrated using a plot of the normalized discharge capacity as a function of cycle number for the purpose of comparison in **Fig. 4a**. Also, the charge and discharge profiles for the first and 100th cycle evaluated at 1C as well as the 101th cycle evaluated at $C/10$ rate are given in **Fig. 4b** and **c**.

Although the both cathodes deliver the initial discharge capacities around 125 mA h g^{-1} at 1C rate, surface-modified cathode exhibits the better capacity retention than pristine cathode with cycling. The ZnAl_2O_4 -coated $\text{LiNi}_{0.5}\text{Mn}_{1.5}\text{O}_4$ delivers the 97.3% of capacity

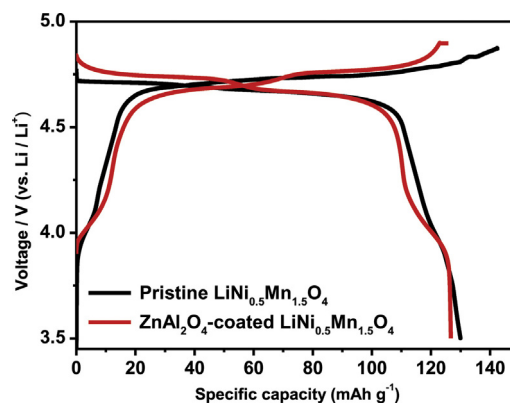


Fig. 3. The charge-discharge voltage profiles at the first cycle for the pristine $\text{LiNi}_{0.5}\text{Mn}_{1.5}\text{O}_4$ and the ZnAl_2O_4 -coated $\text{LiNi}_{0.5}\text{Mn}_{1.5}\text{O}_4$.

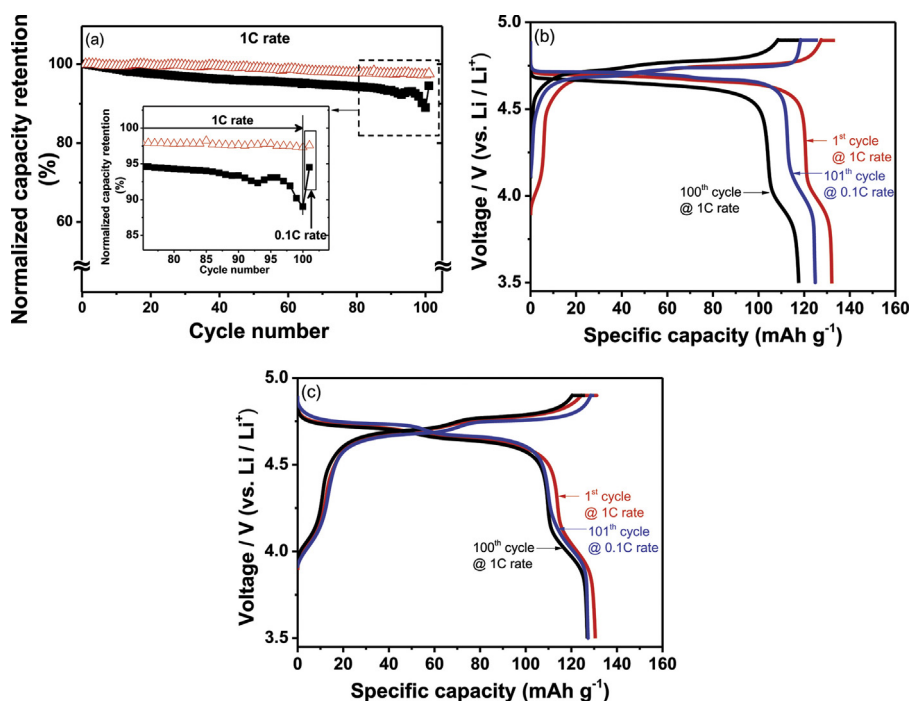


Fig. 4. Comparison of the electrochemical cycling performances at room temperature. (a) Normalized discharge capacity retention at 1C rate: (■) pristine $\text{LiNi}_{0.5}\text{Mn}_{1.5}\text{O}_4$ and (Δ) ZnAl_2O_4 -coated $\text{LiNi}_{0.5}\text{Mn}_{1.5}\text{O}_4$, and charge–discharge voltage profiles of selected cycles for (b) the pristine $\text{LiNi}_{0.5}\text{Mn}_{1.5}\text{O}_4$ and (c) ZnAl_2O_4 -coated $\text{LiNi}_{0.5}\text{Mn}_{1.5}\text{O}_4$.

retention whereas the pristine $\text{LiNi}_{0.5}\text{Mn}_{1.5}\text{O}_4$ retains the 89.0% of initial discharge capacity evaluated at 1C rate after 100 cycles. Interestingly, galvanostatic charge–discharge test at lower C-rate such as C/10 at 101th cycle followed by the 100 cycling test at 1C rate reveals that the capacity retention could be recovered up to 94.5% of initial discharge capacity in the case of the pristine $\text{LiNi}_{0.5}\text{Mn}_{1.5}\text{O}_4$ cathode, implying that the main capacity fade mechanism for the high-voltage $\text{LiNi}_{0.5}\text{Mn}_{1.5}\text{O}_4$ spinel oxides may be attributed to the surface-related phenomenon at solid–electrolyte interface region such as an increase in the ohmic polarization mostly due to the diffusion of Li ion [36]. This result will be discussed in more detail with the XPS analysis.

As the parasitic side reaction between the cathode and the electrolyte can be especially accelerated in the elevated temperature and high-voltage environment [9,26,28,29], the storage test at 60 °C with the fully-charged cathodes for 3 days was performed in the intervals of cycling test evaluated at room temperature in order to confirm and characterize the effect of surface-modification of $\text{LiNi}_{0.5}\text{Mn}_{1.5}\text{O}_4$ cathodes, as shown in Fig. 5. Although the ZnAl_2O_4 -coated electrode maintains its initial capacity during the cycle test at 1C rate after the first storage at 60 °C, the pristine electrode after storage at elevated temperature, on the contrary, shows the unstable behavior during the subsequent cycling at room temperature. Moreover, pristine cathode exhibits the drastic capacity fade after the second storage at elevated temperature, and the 52% of initial discharge capacity (68 mA h g^{-1}) could be only recovered during the subsequent charge–discharge at C/10 rate, implying that the pristine cathode experienced the permanent detriment of active material, especially, in the elevated temperature environment.

Fig. 6 demonstrates the charge–discharge curves and corresponding differential capacity as a function of voltages of pristine and surface-modified cathodes for the selected cycles just before the first storage and after the second storage at 60 °C as previously shown in Fig. 5. Although the slight increase in potential during charge process and the decrease in the capacity values during discharge process can be seen after the storage and cycle test, the

ZnAl_2O_4 -coated cathode maintains the typical charge–discharge profiles as well as the well-distinguished peaks related to the $\text{Ni}^{2+}/\text{Ni}^{4+}$ redox couple, as shown in Fig. 6b [36]. In contrast, for the pristine cathode, elevated temperature and high-voltage environment cause the severe decrease in both the discharge profiles and the corresponding peaks relating to the $\text{Ni}^{2+}/\text{Ni}^{4+}$ redox couple from the dQ/dV profiles, as demonstrated in Fig. 6a. Furthermore, pristine electrode shows the abnormally increased charge capacity after storage test and corresponding peaks in dQ/dV profiles above 4.7 V, which are attributed to the unexpected side reaction between the surface of active materials and the electrolyte.

In order to identify and understand the effect of surface-modification on the electrochemical performances of $\text{LiNi}_{0.5}\text{Mn}_{1.5}\text{O}_4$ oxide materials, XPS spectra of the pristine

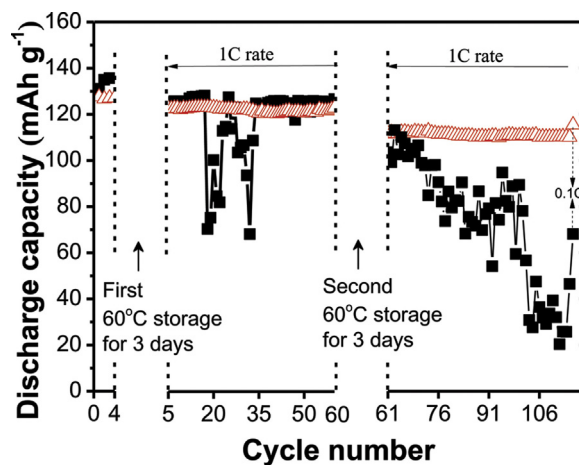


Fig. 5. Comparison of the electrochemical cycling performances combined with the storage test. The storage test was performed at fully charged state and 60 °C: (■) pristine $\text{LiNi}_{0.5}\text{Mn}_{1.5}\text{O}_4$ and (Δ) ZnAl_2O_4 -coated $\text{LiNi}_{0.5}\text{Mn}_{1.5}\text{O}_4$.

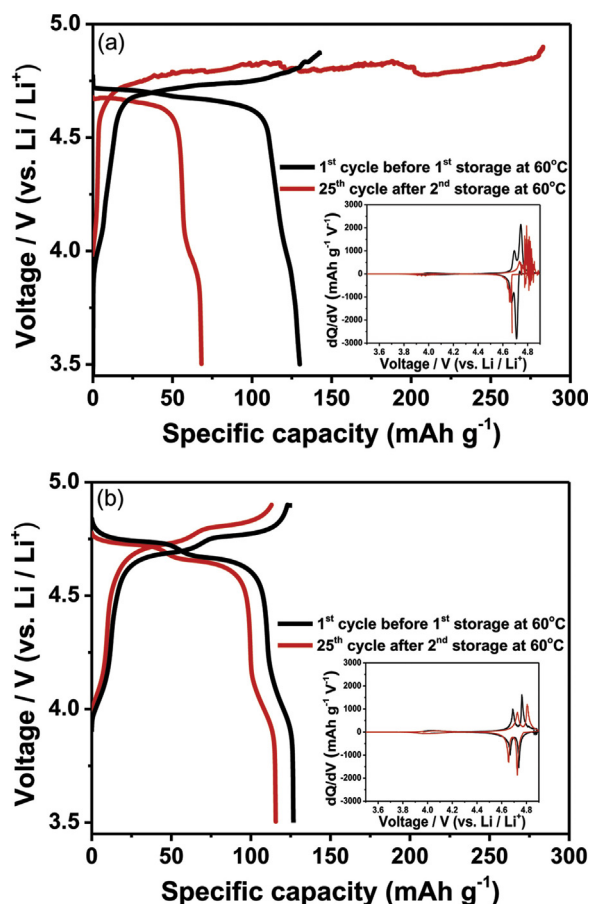


Fig. 6. The charge–discharge voltage profiles at selected cycle. The inset shows the corresponding differential capacity plots as a function of voltages. (a) Pristine $\text{LiNi}_{0.5}\text{Mn}_{1.5}\text{O}_4$ and (b) ZnAl_2O_4 -coated $\text{LiNi}_{0.5}\text{Mn}_{1.5}\text{O}_4$.

and ZnAl_2O_4 -coated cathodes are compared before cycling and after storing the cells at 60°C for 3 days, and the results with peak fitting process are demonstrated in Fig. 7. In the C 1s spectra shown in Fig. 7a, the peak around 286.3 eV after storage test corresponds to residual EC or ROCO₂M formation whereas the peaks around 285.7 and 290.4 eV can be assigned to PVdF binder and Li_2CO_3 species, which is in agreement with previous study [14,37]. Fig. 7b shows the F 1s photoemission peaks, and the peaks around 685 eV are assigned to LiF while the peaks around 687 eV are ascribed to Li_xPF_y and Li_xPOF_y formed by the reaction of LiPF_6 salt [30,37]. Interestingly, F 1s spectra give the significant difference in the peak intensity between the pristine and surface-coated electrodes around 685 eV after storage test, which is assigned to the evidence of LiF. It was reported that the trace amount of H_2O present in the electrolyte result in the formation of HF, which may offend the surface of active material and accelerate the deposition of SEI components such as LiF and LiOH [27,38]. Also, the SEI layer is generally known to be highly resistive. Thus, the growth of LiF layer was effectively suppressed by the surface-coating with ZnAl_2O_4 , leading to the improved electrochemical performances of $\text{LiNi}_{0.5}\text{Mn}_{1.5}\text{O}_4$ cathodes as pointed out earlier.

Fig. 8 shows the DSC profiles of the pristine and ZnAl_2O_4 -coated electrodes evaluated at fully charged state to examine the thermal stability of the cathodes. As demonstrated in Fig. 8, the endothermic and exothermic peaks around 130°C exhibit the solvent decomposition from electrolyte [39,40]. The main exothermic reaction between the cathode and the electrolyte commenced around 165°C , and another exothermic reaction was shown above 260°C . The surface-modified cathode exhibit the increased onset

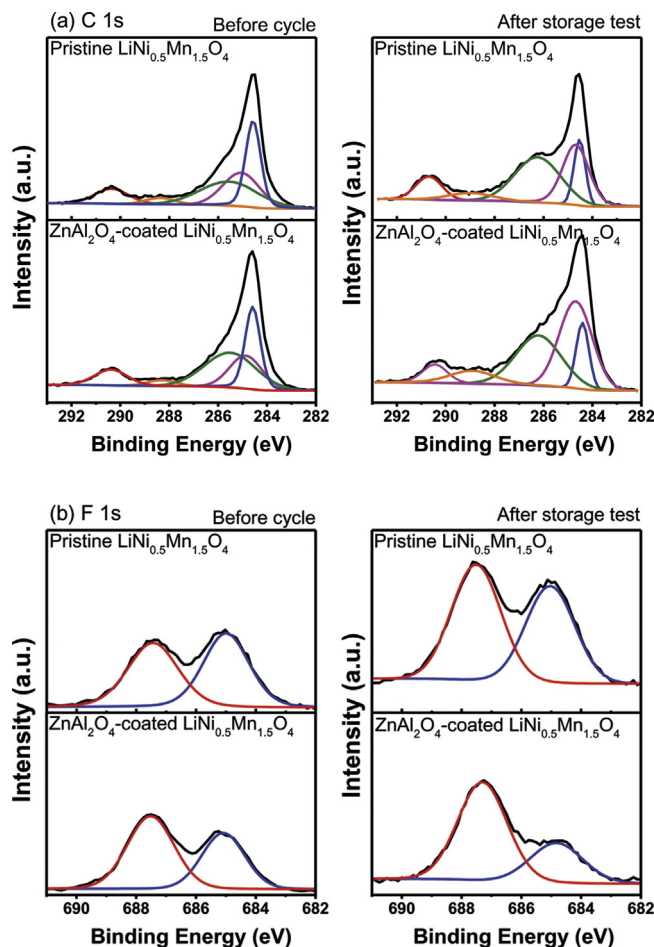


Fig. 7. XPS spectra for (a) C 1s and (b) F 1s for the pristine $\text{LiNi}_{0.5}\text{Mn}_{1.5}\text{O}_4$ and ZnAl_2O_4 -coated $\text{LiNi}_{0.5}\text{Mn}_{1.5}\text{O}_4$ before cycling and after storing the cells at 60°C for 3 days.

peak temperature around 192.1°C and 273.8°C compared to the onset peak temperature of pristine cathode around 181.8°C and 267.1°C , and prominent suppression in reaction enthalpy can be seen for the ZnAl_2O_4 -coated cathode. The reaction enthalpy values above 130°C for the pristine and ZnAl_2O_4 -coated electrodes were 864.7 J g^{-1} and 528.3 J g^{-1} , respectively, suggesting that the ZnAl_2O_4 -coating improves the thermal stability of the high-voltage cathode materials, which consequently lead to the lower reactivity with electrolyte.

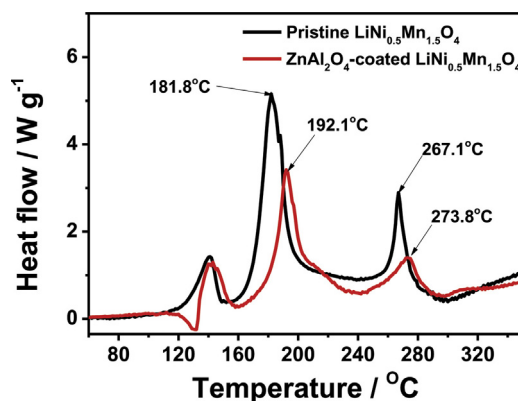


Fig. 8. DSC profiles of the pristine $\text{LiNi}_{0.5}\text{Mn}_{1.5}\text{O}_4$ and ZnAl_2O_4 -coated $\text{LiNi}_{0.5}\text{Mn}_{1.5}\text{O}_4$.

4. Conclusion

Spinel $\text{LiNi}_{0.5}\text{Mn}_{1.5}\text{O}_4$ powders were coated with ZnAl_2O_4 using a sol–gel method to improve the electrochemical performances as well as the thermal stability. The ZnAl_2O_4 -coated $\text{LiNi}_{0.5}\text{Mn}_{1.5}\text{O}_4$ cathodes showed the enhanced capacity retention evaluated at 1C rate cycling test at room temperature mostly due to the suppressed ohmic polarization compared to the pristine $\text{LiNi}_{0.5}\text{Mn}_{1.5}\text{O}_4$ cathodes. Furthermore, surface-modified cathodes recovered the 87% of initial capacity after the 1C rate cycling test combined with the storage test at fully charged state and 60 °C whereas the pristine cathodes delivered the only the 52% of its initial capacity. The DSC analysis indicates that the surface-coating also leads to the significant improvement in thermal stability of cathode materials. The excellent electrochemical performances are thought to be originated from the suppressed LiF formation on the surface of cathodes in the XPS study.

Acknowledgement

This work was supported by the National Research Foundation of Korea Grant funded by the Korean Government (MEST) (NRF-2010-C1AAA001-2010-0028958).

References

- [1] J.M. Tarascon, M. Armand, Issues and challenges facing rechargeable lithium batteries, *Nature* 414 (2001) 359.
- [2] M. Winter, J.O. Besenhard, M.E. Spahr, P. Novak, Insertion electrode materials for rechargeable lithium batteries, *Adv. Mater.* 10 (1998) 725.
- [3] M.M. Thackeray, P.J. Johnson, L.A. de Piccolto, P.G. Bruce, J.B. Goodenough, Electrochemical extraction of lithium from LiMn_2O_4 , *Mater. Res. Bull.* 19 (1984) 179.
- [4] M.S. Whittingham, Lithium batteries and cathode materials, *Chem. Rev.* 104 (2004) 4271.
- [5] K.M. Shaju, P.G. Bruce, Macroporous $\text{Li}(\text{Ni}_{1/3}\text{Co}_{1/3}\text{Mn}_{1/3})\text{O}_2$: a high-power and high-energy cathode for rechargeable lithium batteries, *Adv. Mater.* 18 (2006) 2330.
- [6] A.K. Padhi, K.S. Najundswamy, J.B. Goodenough, Phospho-olivines as positive-electrode materials for rechargeable lithium batteries, *J. Electrochem. Soc.* 144 (1997) 1188.
- [7] Y. Idemoto, H. Narai, N. Koura, Crystal structure and cathode performance dependence on oxygen content of $\text{LiMn}_{1.5}\text{Ni}_{0.5}\text{O}_4$ as a cathode material for secondary lithium batteries, *J. Power Sources* 119–121 (2003) 125.
- [8] Y. Sun, Z. Wang, X. Huang, L. Chen, Synthesis and electrochemical performance of spinel $\text{LiMn}_{2-x-y}\text{Ni}_x\text{Cr}_y\text{O}_4$ as 5-V cathode materials for lithium ion batteries, *J. Power Sources* 132 (2004) 161.
- [9] Y. Talyosef, B. Markovsky, G. Salitra, D. Aurbach, H.-J. Kim, S. Choi, The study of $\text{LiNi}_{0.5}\text{Mn}_{1.5}\text{O}_4$ 5-V cathodes for Li-ion batteries, *J. Power Sources* 146 (2005) 664.
- [10] T. Ohzuku, S. Takeda, M. Iwanaga, Solid-state redox potentials for $\text{Li}[\text{Me}_{1/2}\text{Mn}_{3/2}]\text{O}_4$ (Me: 3d-transition metal) having spinel-framework structures: a series of 5 volt materials for advanced lithium-ion batteries, *J. Power Sources* 81–82 (1999) 90.
- [11] X.X. Xu, J. Yang, Y.Q. Wang, Y.N. NuLi, J.L. Wang, $\text{LiNi}_{0.5}\text{Mn}_{1.5}\text{O}_{3.975}\text{F}_{0.05}$ as novel 5V cathode material, *J. Power Sources* 174 (2007) 1113.
- [12] T.A. Arunkumar, A. Manthiram, Influence of lattice parameter differences on the electrochemical performance of the 5V spinel $\text{LiMn}_{1.5-y}\text{Ni}_{0.5-z}\text{Mg}_{y+z}\text{O}_4$ (M = Li, Mg, Fe, Co, and Zn), *Electrochem. Solid-State Lett.* 8 (2005) A403.
- [13] T.A. Arunkumar, A. Manthiram, Influence of chromium doping on the electrochemical performance of the 5V spinel cathode $\text{LiMn}_{1.5}\text{Ni}_{0.5}\text{O}_4$, *Electrochim. Acta* 50 (2005) 5568.
- [14] H. Duncan, D. Duguay, Y. Abu-Lebdeh, I.J. Davidson, Study of the $\text{LiMn}_{1.5}\text{Ni}_{0.5}\text{O}_4$ /electrolyte interface at room temperature and 60 °C, *J. Electrochem. Soc.* 158 (2011) A537.
- [15] D. Aurbach, B. Markovsky, Y. Talyosef, G. Salitra, H.-J. Kim, S. Choi, Studies of cycling behavior, ageing, and interfacial reactions of $\text{LiNi}_{0.5}\text{Mn}_{1.5}\text{O}_4$ and carbon electrodes for lithium-ion 5-V cells, *J. Power Sources* 162 (2006) 780.
- [16] Y. Talyosef, B. Markovsky, R. Lavi, G. Salitra, D. Aurbach, D. Kovacheva, M. Gorova, E. Zhecheva, R. Stoyanova, Comparing the behavior of nano- and micro-sized particles of $\text{LiMn}_{1.5}\text{Ni}_{0.5}\text{O}_4$ spinel as cathode materials for Li-ion batteries, *J. Electrochem. Soc.* 154 (2007) A682.
- [17] U. Lafont, C. Locati, W.J.H. Borghols, A. Lasinska, J. Dygas, A.V. Chadwick, E.M. Kelder, Nanosized high voltage cathode material $\text{LiMg}_{0.05}\text{Ni}_{0.45}\text{Mn}_{1.5}\text{O}_4$: structural, electrochemical and in situ investigation, *J. Power Sources* 189 (2009) 179.
- [18] R. Santhanam, B. Rambabu, Research progress in high voltage spinel $\text{LiNi}_{0.5}\text{Mn}_{1.5}\text{O}_4$ material, *J. Power Sources* 195 (2010) 5442.
- [19] B. Markovsky, Y. Talyosef, G. Salitra, D. Aurbach, H.-J. Kim, S. Choi, Cycling and storage performance at elevated temperatures of $\text{LiNi}_{0.5}\text{Mn}_{1.5}\text{O}_4$ positive electrodes for advanced 5V Li-ion batteries, *Electrochem. Commun.* 6 (2004) 821.
- [20] C. Li, Y. Zhao, H. Zhang, J. Liu, J. Jing, X. Cui, S. Li, Compatibility between $\text{LiNi}_{0.5}\text{Mn}_{1.5}\text{O}_4$ and electrolyte based upon lithium bis(oxalate)borate and sulfonate for high voltage lithium-ion batteries, *Electrochim. Acta* 104 (2013) 134.
- [21] T. Yang, N. Zhang, Y. Lang, K. Sun, Enhanced rate performance of carbon-coated $\text{LiNi}_{0.5}\text{Mn}_{1.5}\text{O}_4$ cathode material for lithium ion batteries, *Electrochim. Acta* 56 (2011) 4058.
- [22] Y. Wang, G. Yang, Z. Yang, L. Zhang, M. Fu, H. Long, Z. Li, Y. Huang, P. Lu, High power and capacity of $\text{LiNi}_{0.5}\text{Mn}_{1.5}\text{O}_4$ thin films cathodes prepared by pulsed laser deposition, *Electrochim. Acta* 102 (2013) 416.
- [23] Y.-C. Jin, C.-Y. Lin, J.-G. Duh, Improving rate capability of high potential $\text{LiNi}_{0.5}\text{Mn}_{1.5}\text{O}_{4-x}$ cathode materials via increasing oxygen non-stoichiometries, *Electrochim. Acta* 69 (2012) 45.
- [24] I. Kishida, K. Orita, A. Nakamura, Y. Yokogawa, Thermodynamic analysis using first-principles calculations of phases and structures of $\text{Li}_x\text{Ni}_{0.5}\text{Mn}_{1.5}\text{O}_4$ ($0 \leq x \leq 1$), *J. Power Sources* 241 (2013) 1.
- [25] S.-Y. Ha, J.-G. Han, Y.-M. Song, M.-J. Chun, S.-I. Han, W.-C. Shin, N.-S. Choi, Using a lithium bis(oxalato) borate additive to improve electrochemical performance of high-voltage spinel $\text{LiNi}_{0.5}\text{Mn}_{1.5}\text{O}_4$ cathodes at 60 °C, *Electrochim. Acta* 104 (2013) 170.
- [26] J.C. Arrebola, A. Caballero, L. Hernan, J. Morales, Re-examining the effect of ZnO on nanosized 5V $\text{LiNi}_{0.5}\text{Mn}_{1.5}\text{O}_4$ spinel: an effective procedure for enhancing its rate capability at room and high temperatures, *J. Power Sources* 195 (2010) 4278.
- [27] J. Liu, A. Manthiram, Understanding the improvement in the electrochemical properties of surface modified 5V $\text{LiMn}_{1.42}\text{Ni}_{0.42}\text{Co}_{0.16}\text{O}_4$ spinel cathodes in lithium-ion cells, *Chem. Mater.* 21 (2009) 1695.
- [28] H.M. Wu, I. Belharouak, A. Abouimrane, Y.-K. Sun, K. Amine, Surface modification of $\text{LiNi}_{0.5}\text{Mn}_{1.5}\text{O}_4$ by ZrP_2O_7 and ZrO_2 for lithium-ion batteries, *J. Power Sources* 195 (2010) 2909.
- [29] J. Liu, A. Manthiram, Kinetics study of the 5V spinel cathode $\text{LiMn}_{1.5}\text{Ni}_{0.5}\text{O}_4$ before and after surface modifications, *J. Electrochem. Soc.* 156 (2009) A833.
- [30] Y. Fan, J. Wang, Z. Tang, W. He, J. Zhang, Effects of the nanostructured SiO_2 coating on the performance of $\text{LiNi}_{0.5}\text{Mn}_{1.5}\text{O}_4$ cathode materials for high-voltage Li-ion batteries, *Electrochim. Acta* 52 (2007) 3870.
- [31] H.-B. Kang, S.-T. Myung, K. Amine, S.-M. Lee, Y.-K. Sun, Improved electrochemical properties of BiOF-coated 5V spinel $\text{Li}[\text{Ni}_{0.5}\text{Mn}_{1.5}]\text{O}_4$ for rechargeable lithium batteries, *J. Power Sources* 195 (2010) 2023.
- [32] M. Zawadzki, Synthesis of nanosized and microporous zinc aluminate spinel by microwave assisted hydrothermal method (microwave-hydrothermal synthesis of ZnAl_2O_4), *Solid State Sci.* 8 (2006) 14.
- [33] S. Shen, K. Hidajat, L.E. Yu, S. Kawi, Simple hydrothermal synthesis of nanostructured and nanorod Zn–Al complex oxides as novel nanocatalysts, *Adv. Mater.* 16 (2004) 541.
- [34] K.K. Satapathy, F. Khan, Influence of the fuels on the mechanoluminescence properties of Dy doped ZnAl_2O_4 phosphors, *Chem. Mater. Res.* 2 (2012) 23.
- [35] S. Mathur, M. Veith, M. Haas, H. Shen, N. Lerb, V. Huch, Single-source sol–gel synthesis of nanocrystalline ZnAl_2O_4 : structural and optical properties, *J. Am. Ceram. Soc.* 84 (2001) 1921.
- [36] D. Liu, J. Han, J.B. Goodenough, Structure, morphology, and cathode performance of $\text{Li}_{1-x}[\text{Ni}_{0.5}\text{Mn}_{1.5}\text{O}_4]$ prepared by coprecipitation with oxalic acid, *J. Power Sources* 195 (2010) 2918.
- [37] H. Duncan, Y. Abu-Lebdeh, I.J. Davidson, Study of the cathode–electrolyte interface of $\text{LiMn}_{1.5}\text{Ni}_{0.5}\text{O}_4$ synthesized by a sol–gel method for Li-ion batteries, *J. Electrochem. Soc.* 157 (2010) A528.
- [38] S. Myung, K. Izumi, S. Komaba, Y. Sun, H. Yashiro, N. Kumagai, Role of alumina coating on Li–Ni–Co–Mn–O particles as positive electrode material for lithium-ion batteries, *Chem. Mater.* 17 (2005) 3695.
- [39] T. Nukuda, T. Inamasu, A. Fujii, D. Endo, H. Nakagawa, S. Kozono, T. Iguchi, J. Kuratomi, K. Kohno, S. Izuchi, M. Oshitani, Development of a lithium ion battery using a new cathode material, *J. Power Sources* 146 (2005) 611.
- [40] S.H. Kang, J. Kim, M.E. Stoll, D. Abraham, Y.-K. Sun, K. Amine, Layered $\text{Li}(\text{Ni}_{0.5-x}\text{Mn}_{0.5-x}\text{M}_2\text{x}')\text{O}_2$ ($\text{M}' = \text{Co, Al, Ti}$; $x = 0, 0.025$) cathode materials for Li-ion rechargeable batteries, *J. Power Sources* 41 (2002) 112.